

Supporting Information

Fast self-charging and temperature adaptive electrochromic energy storage device

Yue Wang, Xiaolan Zhong, Xueqing Liu, Zelin Lu, Yingjie Su, Mengying Wang, and Xungang Diao*

Content of Supporting Information

1. Transmittance in the visible range of the PAAm-7.5 M ZnCl₂
2. Self-charging rate comparison with other electrochromic self-rechargeable batteries
3. The redox reaction of PANI
4. Digital photos of the ECESD showing different colors when different voltages are applied
5. The color change of ECESD under different voltages when the bending radius is 1.5 cm
6. CV curves of the ECESD at -25°C and 50°C at different sweep speeds
7. Reflection spectra of the ECESD in charge and discharge states at different temperatures.
8. Electrochemical impedance spectroscopy of PAAm-7.5 M ZnCl₂ gel at different temperatures
9. References

1. Transmittance in the visible range of the PAAm-7.5 M ZnCl₂

As shown in Fig. S1, the hydrogel electrolyte showed an average transmittance of

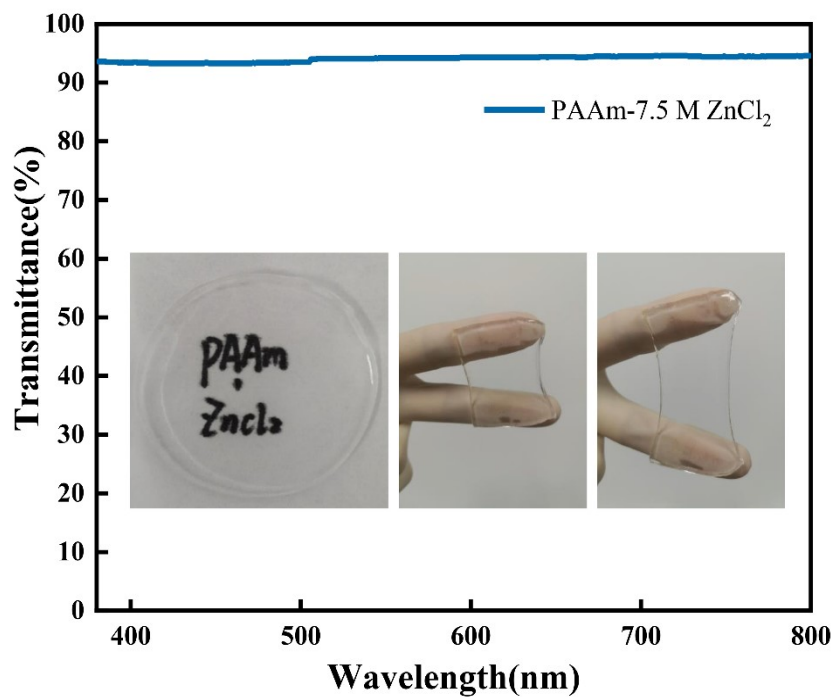


Fig. S1. Transmittance in the visible range of the PAAm-7.5 M ZnCl₂ 94.1% in the visible range (wavelength 380 to 800 nm).

2. Self-charging rate comparison with other electrochromic self-rechargeable batteries

Define the ratio of battery self-charging capacity recovery percentage to self-charging time (h) as the battery self-charging rate. Fig. S2 shows the comparison between the self-charging rate of ECESD and other electrochromic self-charging

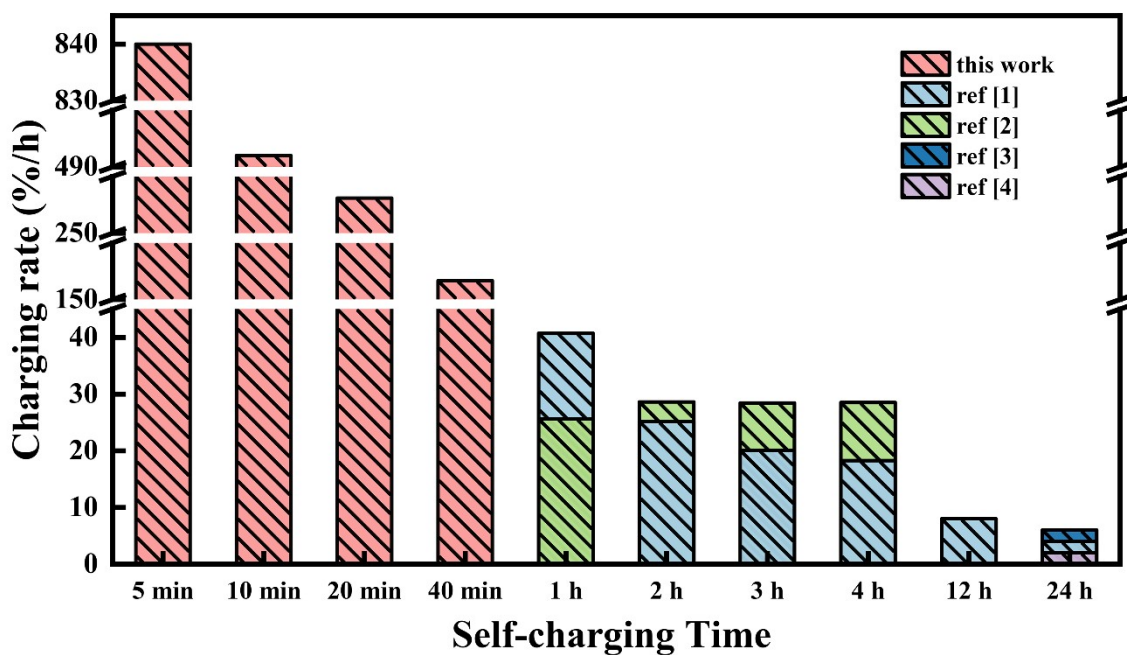


Fig. S2. Self-charging rate comparison with other electrochromic self-rechargeable batteries energy storage devices, indicating that ECESD has fast self-charging capability

3. The redox reaction of PANI

Fig. S3a presented the CV curves of PANI under different scan rate in 7.5 M ZnCl₂ electrolyte solution. The CV behaviors demonstrated two pairs of typical redox peaks at positive potentials. The oxidation peak at 0.176 V and reduction peak -0.185 V at a scanning speed of 10 mV s⁻¹ in Fig. S3a corresponds to the change between LB and ES with anion doping upon oxidation and dedoping upon reduction to compensate the charge of the PANI film, respectively. Their simplified reaction is shown in Equation 1 of Fig. S3b. The oxidation peak at 0.735 V and reduction peak 0.250 V correspond to the conversion between EB and PS with doping and dedoping of the anion processes,

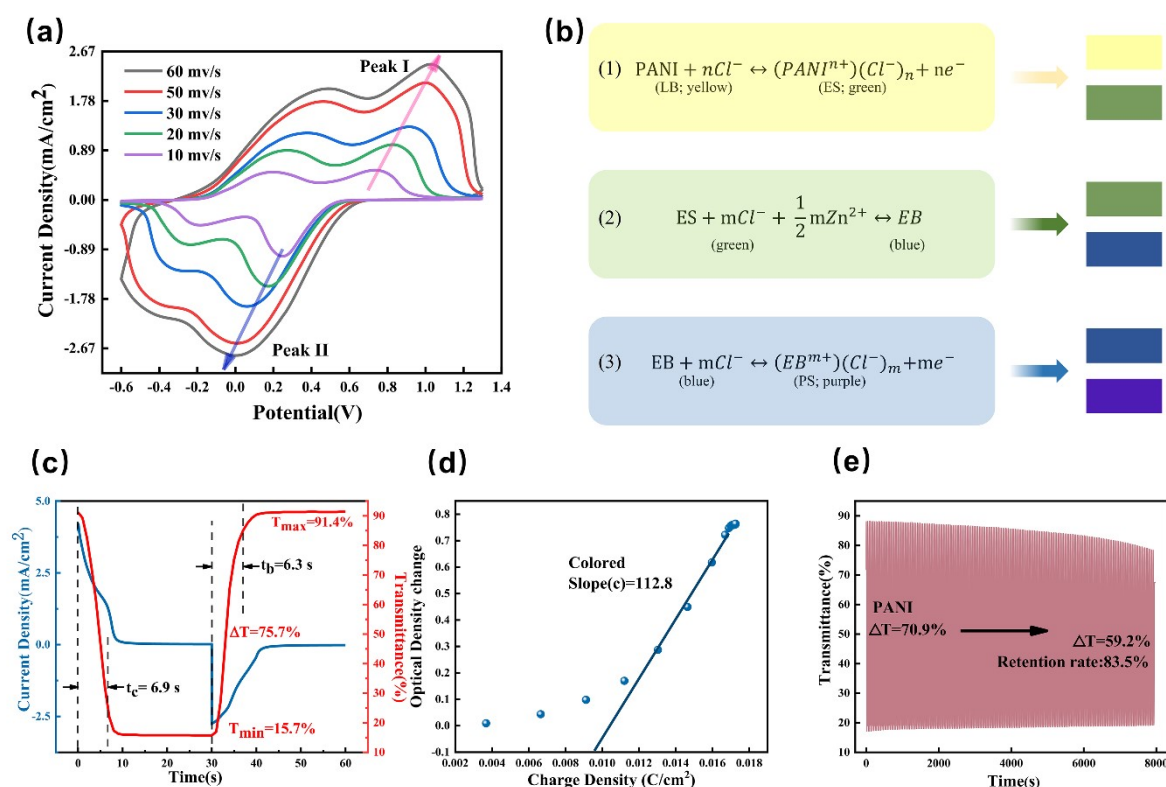


Fig. S3. (a) CV curves of PANI electrodes at different scan rates. (b) The redox reaction of PANI. (c) Variation in current density (blue curves) and transmittance (red curves) and switching time characteristics between the colored and bleached states for PANI films in 7.5 M ZnCl₂ electrolyte solution measured at -0.6 V and +1.3 V for 30 s at a wavelength of 550 nm. (d) The Coloration efficiency of the PANI. (e) Life cycle measurements for the PANI with CV measurement for -0.6 V~+1.3 V and the sweep rate is 100 mV s⁻¹.

respectively, and their simplified reaction is shown in Equation 3 of Fig. S3b. (The abbreviation for the above is: the fully reduced leucoemeraldine (LB) form (transparent yellow), the 50% oxidized emeraldine salt (ES) form (green), the emeraldine base (EB)

form (blue), and the fully oxidized pernigraniline (PS) form (purple)).

Concerning the switching kinetics of PANI films in 7.5 M ZnCl₂ electrolyte solution, the chronoamperometry (CA) technique was used by applying alternant potential of -0.2 V and +1.3 V for 30 s with the in-situ optical transmittance measurement at a wavelength of 550 nm. The second CA cycle data and corresponding transmittance variation curves were recorded and displayed in Fig. S3c. Generally, the colored and bleached switching time was defined as the time required to achieve 90% of final optical modulation during coloring and bleaching process, which denoted as t_c and t_b , respectively. The films measured in 7.5 M ZnCl₂ showed switching times of 6.9 s for coloring process (t_c) and 6.3 s for bleaching process (t_b). At the same time, the coloration efficiency is an important parameter to evaluate the EC performance, which was defined as the change in optical density per unit of inserted charge density,

$$CE = \frac{\Delta OD}{q} = \log \left(\frac{T_b}{T_c} \right) / q$$

where q is the inserted and extracted charges per area, optical density $\Delta OD = \log (T_b/T_c)$ is determined by the transmittance in bleached state (T_b) and colored state (T_c). The CE values were calculated from the CA and in-situ optical transmittance variations (Fig. S3c), and the CE value is as high as 112.8 cm² C⁻¹ (Fig. S3d).

We further studied the cyclic stability of PANI film, and the cyclic stability of PANI was measured by CV technique. Fig. S3e shows the optical transmittance modulation change of the PANI film under 8000 s CV test. It can be found that the ΔT of the PANI film decreased from 70.9% of the initial value to 59.2% after 8000 s, and the retention rate was 83.5%, without significant degradation.

4. Digital photos of the ECESD showing different colors when different voltages are applied

the ECESD was fabricated into a sandwiched structure with the PANI electrode, hydrogel electrolyte and Zn electrode. Cyclic voltammetry (CV) scanning in the range of 0.2–1.5 V was applied to the two electrodes. The PANI electrode on the top exhibited a purple color at 1.5 V, which was bleached gradually to “blue → green → light yellow” when the voltage swiping to 0.2 V (Fig. S4).

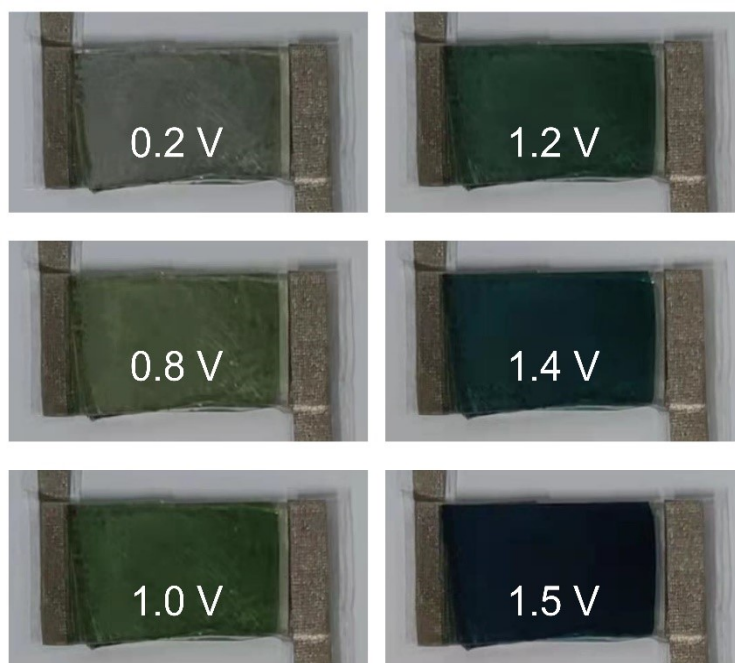


Fig. S4. Digital photos of the ECESD showing different colors when different voltages are applied

5. The color change of ECESD under different voltages when the bending radius is 1.5 cm

As shown in Fig. S5, the ECESD at bent state also exhibited an obvious coloring and discoloration phenomenon, demonstrating excellent flexibility.

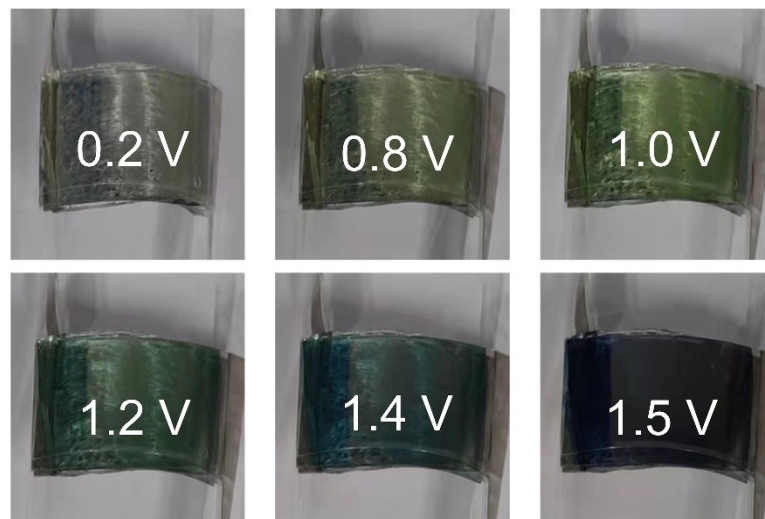


Fig. S5. The color change of ECESD under different voltages when the bending radius is 1.5 cm

6. CV curves of the ECESD at -25°C and 50°C at different sweep speeds

As the scan rate increases, the CV curve basically maintains a similar shape at -25°C and 50°C, indicating that the device has excellent electrochemical reversibility at both low and high temperatures (Fig. S6).

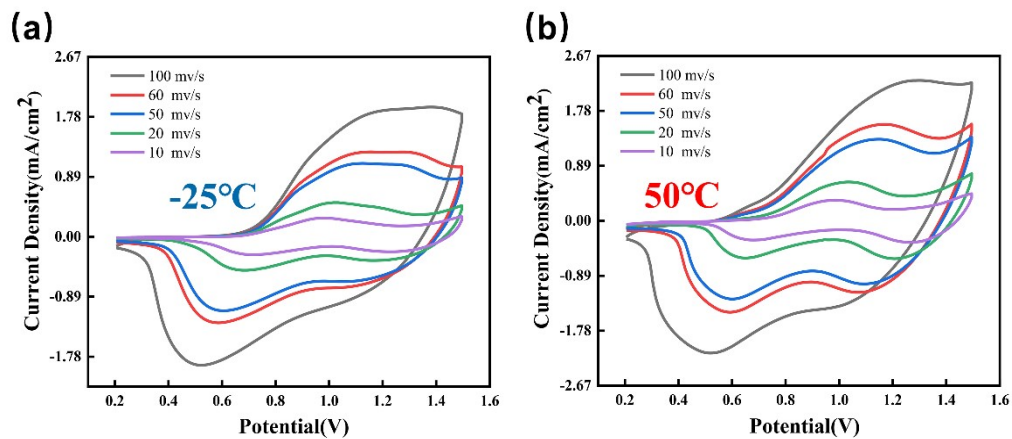


Fig. S6 CV curves of the ECESD at -25°C and 50°C at different sweep speeds

7. Reflection spectra of ECESD in charge and discharge states at different temperatures.

In order to represent the response of reflection spectrum at different temperatures, we kept the device at -25°C , 0°C , 25°C , and 50°C for 15 minutes and then measure the reflectance spectrum of the device at -0.2 V and 1.5 V , which showed that the ECESD will undergo an obvious color transition even in the process of charging and discharging at high and low temperatures (Fig. S7).

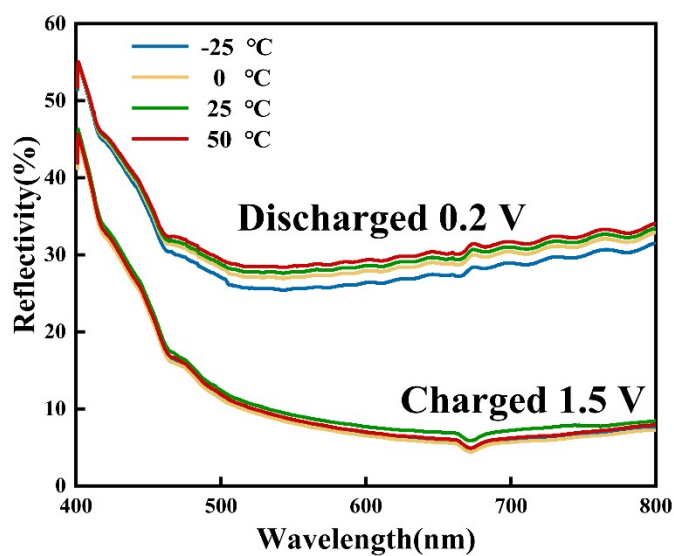


Fig. S7. Reflection spectra of ECESD in charge and discharge states at different temperatures.

8. Electrochemical impedance spectroscopy of PAAm-7.5 M ZnCl₂ gel at different temperatures

As shown in Fig. S6, the intercept between the straight line and the horizontal axis is the self-resistance of the electrolyte. It can be seen that the bulk resistance value is almost the same at -25°C and 25°C, which proves that PAAm-7.5 M ZnCl₂ still has high ionic conductivity at low temperatures. As the temperature increases, the self-resistance decreases. At 50°C, the self-resistance decreases significantly, indicating that the increase in temperature accelerates the ion migration rate, which is consistent with the previous experimental results.

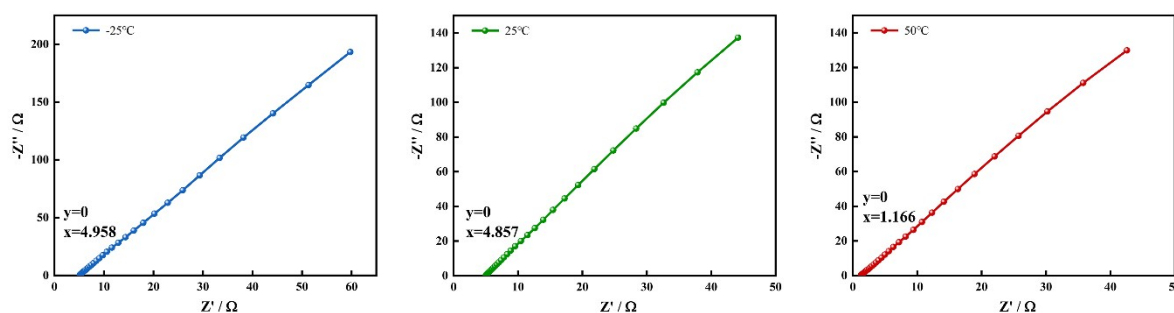


Fig. S8. Electrochemical impedance spectroscopy of PAAm-7.5 M ZnCl₂ gel at different

9. References

1. B. Yang, D. Ma, E. Zheng and J. Wang, *Solar Energy Materials and Solar Cells*, 2019, **192**, 1-7.
2. X. Chang, R. Hu, S. Sun, J. Liu, Y. Lei, T. Liu, L. Dong and Y. Yin, *Applied Surface Science*, 2018, **441**, 105-112.
3. H. Li, L. McRae, C. J. Firby and A. Y. Elezzabi, *Advanced Materials*, 2019, **31**.
4. J. Wang, L. Zhang, L. Yu, Z. Jiao, H. Xie, X. W. Lou and X. W. Sun, *Nature Communications*, 2014, **5**.